



Contents lists available at ScienceDirect

Nuclear Instruments and Methods in Physics Research A

journal homepage: www.elsevier.com/locate/nima

Ion beam heated target simulations for warm dense matter physics and inertial fusion energy [☆]

J.J. Barnard ^{a,*}, J. Armijo ^b, D.S. Bailey ^a, A. Friedman ^a, F.M. Bieniosek ^b, E. Henestroza ^b, I. Kaganovich ^c, P.T. Leung ^e, B.G. Logan ^b, M.M. Marinak ^a, R.M. More ^b, S.F. Ng ^{b,e}, G.E. Penn ^b, L.J. Perkins ^a, S. Veitzer ^d, J.S. Wurtele ^b, S.S. Yu ^{b,e}, A.B. Zylstra ^b

^a Lawrence Livermore National Laboratory, Livermore, CA 94550, USA

^b Lawrence Berkeley National Laboratory, Berkeley, CA 94720, USA

^c Princeton Plasma Physics Laboratory, Princeton, NJ 08543, USA

^d Tech-X Corporation, Boulder, CO 80303, USA

^e Chinese University of Hong Kong, Hong Kong, China

ARTICLE INFO

Available online 5 April 2009

Keywords:

Ion beam heating
Warm dense matter
Inertial fusion energy targets
Hydrodynamic simulation

ABSTRACT

Hydrodynamic simulations have been carried out using the multi-physics radiation hydrodynamics code HYDRA and the simplified one-dimensional hydrodynamics code DISH. We simulate possible targets for a near-term experiment at LBNL (the Neutralized Drift Compression Experiment, NDCX) and possible later experiments on a proposed facility (NDCX-II) for studies of warm dense matter and inertial fusion energy-related beam-target coupling. Simulations of various target materials (including solids and foams) are presented. Experimental configurations include single-pulse planar metallic solid and foam foils. Concepts for double-pulsed and ramped-energy pulses on cryogenic targets and foams have been simulated for exploring direct drive beam-target coupling, and concepts and simulations for collapsing cylindrical and spherical bubbles to enhance temperature and pressure for warm dense matter studies.

© 2009 Elsevier B.V. All rights reserved.

1. Introduction

Heavy ion accelerators have long been advanced as drivers for inertial fusion energy (IFE) for their high efficiency, intrinsically high repetition rate, and their attractive final focus and chamber solutions. In a heavy ion fusion (HIF) driver, the final focus is accomplished using magnets (quadrupoles or solenoids), which can be shielded from the fusion microexplosions. The solid chamber wall can be shielded from the microexplosions using a flowing liquid salt that acts as protection to the solid wall, an absorber of heat from the microexplosion, a heat transfer medium, and a breeder of the tritium component of the fuel. Because of high accelerator efficiency, both indirect drive targets and direct drive targets remain options for HIF. Indirect drive has relatively low intrinsic coupling efficiency (ratio of fuel kinetic energy to beam energy) because of the energy penalty in increasing the temperature of the hohlraum walls, but indirect drive targets have intrinsically high uniformity in capsule

illumination and are of practical importance because they will be the first types of targets to be studied on the National Ignition Facility (NIF) using laser beams. Direct drive targets potentially have high capsule coupling efficiency, but high capsule illumination uniformity must be achieved by large beam number or other means. To date, most work on HIF targets has been for indirect drive, but recently direct drive is being reexamined as a potential means of increasing target gain (ratio of fusion yield to beam energy), reducing the scale of the driver [1].

Recently, high-energy density physics (HEDP) and warm dense matter (WDM) have received interest for its potential for fundamental physics discovery as well as its applications to astrophysics and inertial confinement fusion (ICF) [2]. Heavy ion accelerators also have some advantages for HEDP/WDM as well as for IFE. In particular, ions deposit their energy in a material volumetrically over macroscopic volumes (microns to millimeters, depending on the ion mass and energy). Secondly, there are several energies where the ion energy loss rate (dE/dX) is nearly constant (for example, at the Bragg peak), so that the deposition may be arranged to be nearly uniform over regions that can be macroscopically diagnosed. In the US, high-current low-energy accelerators are currently exploiting the plateau in dE/dX from nuclear stopping on the Neutralized Drift Compression Experiment (NDCX-I) [3] and plans are being developed to exploit

[☆] Work performed under the auspices of the US Department of Energy under Contract DE-AC52-07NA27344 at LLNL, and University of California Contract DE-AC02-05CH11231 at LBNL and Contract DEFG0295ER40919 at PPPL.

* Corresponding author.

E-mail address: jjbarnard@llnl.gov (J.J. Barnard).

deposition at the Bragg peak on an upgrade called NDCX-II. This is in contrast to the European approach at GSI using high-energy but lower current accelerators that operate near a minimum in dE/dX providing large volumes of uniform energy deposition [4,5]. Ideally the energy deposition occurs in a time that is short compared to the hydro expansion time scale, so that temperatures larger compared to the vaporization temperature can be achieved but at solid density. Recently, NDCX-I has been used to study beam compression to short pulse durations and simultaneously small focal spots. Plasma is introduced along the beam path [6,7] to reduce the effects of space charge both longitudinally (to minimize pulse duration) and radially (to minimize spot radius). Although initially a beam physics experiment, a target chamber has been designed, fabricated and installed and a suite of diagnostics has been developed and is being tested on NDCX-1. The target temperatures that will be achieved on NDCX-I depend ultimately on the central beam intensity, and experiments in the metallic two-phase regime are expected to be carried out soon [8].

In this paper, we describe simulations of experiments that are relevant to recent developments in both HIF and WDM. In Section 2, we list some of the parameters expected for NDCX-I and describe simulations carried out in support of the experiment. In Section 3, we discuss simulations for targets of a planned accelerator, which would have significantly more ion energy and current than NDCX-I, called NDCX-II [9], and that would operate at or near the Bragg peak where the derivative of the energy loss rate (dE/dX) with respect to energy is zero. The targets include planar solids and metallic foams, and foils with cylindrical and spherical bubbles embedded within them. In Section 3, we briefly discuss a concept for ion-driven direct drive for IFE, and in Section 4, we describe the concepts for and simulations of experiments on NDCX-II, which would help validate aspects of the direct drive target concepts discussed in Section 3.

2. NDCX-I planar targets

NDCX-I currently produces a 350 kV, 25 mA singly charged potassium ion beam with a pulse duration up to $10 \mu\text{s}$ [3]. Four solenoids provide beam confinement and impart a radial convergence towards a final, high-field solenoid. A section of the beam, approximately 120 ns in length, can receive a time-dependent voltage ramp that gives the tail a velocity increase relative to the head, which, in the absence of space charge effects, can compress the pulse to a duration of ~ 2 ns and a current of approximately 2 A. After the voltage tilt is imposed, the beam passes into a neutralized drift section where plasma is injected along the path of the beam. After the 2 m drift, the beam passes through a final solenoid where it converges towards the target to a radius ($2^{1/2}$ rms) of 0.5–2 mm. Fig. 1 shows the results from HYDRA [10] simulations (by E. Henestroza) of the beam impinging on a 300 nm tin foil after 6 ns. As can be seen in the simulation, the temperature reaches approximately 0.24 eV. By using the prepulse to heat the material near (or to) the boiling point, and then depositing a short (~ 2 ns) pulse to super critically raise the temperature of the material, optimal use of the total pulse energy may be obtained and observations of the material expanding through the two-phase region may be achieved. A gold cone (cf [8]) to focus the beam will be employed to further enhance the beam intensity, as well as to ensure that the beam is fully neutralized near the target. The ion energy of NDCX-I will be below the energy at the Bragg peak, but nevertheless will be relatively constant due to the plateau in dE/dX with energy at that energy arising from contributions to nuclear scattering. Descriptions of the experiments planned on NDCX-I may be found in [8]. Part of the evolution of the expanding material will

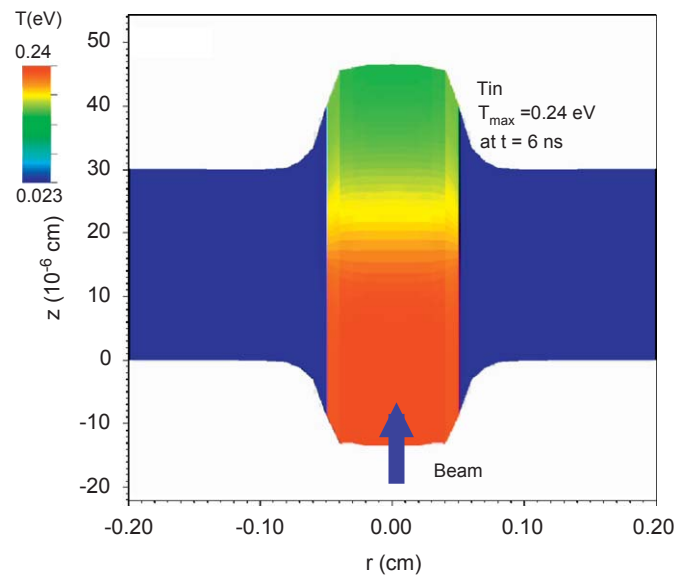


Fig. 1. HYDRA simulation of NDCX-I beam focused onto 300 nm tin foil. Color indicates the temperature at points within the foil, 6 ns after the NDCX-I beam began bombarding the foil. Parameters used in the simulation: Ion energy 350 keV, ion species: K^+ , spot radius 0.5 mm, central peak fluence of 0.1 J/cm^2 .

be through the two-phase (vapor/liquid) regime, and the evolution of the droplets and bubbles in super-heated metals is of practical interest [11]. The droplet evolution has been modeled using simple kinetic rate equations, which suggest that most droplets should persist in the outflowing expanding material. See e.g. [11,12].

3. NDCX-II targets for WDM

With the higher ion energy (~ 2.8 MeV), ion current (~ 30 A), longer range ($\sim 4 \mu\text{m}$) and shorter pulse (~ 1 ns FWHM), NDCX-II is being designed for experiments in the WDM regime, i.e. it will be able to access temperatures around the critical temperature of several metals (~ 1 eV), and densities at solid density and below. Simulations [13] of the NDCX-II beam impinging upon a solid or foam target of Al have shown that pressures slightly less than 1 Mbar will be achieved in solids, and less in foams. To achieve even higher pressures and temperatures with the same ion beam, novel target configurations are being considered. One such technique utilizes voids in the material to allow the pressure from heated walls surrounding the voids to compress the material between the expanding metallic walls. Planar voids, cylindrical holes and spherical holes are being considered. The highest temperatures and pressures so far achieved to date in the simulations using NDCX-II parameters occur when spherical bubbles (containing Ar gas) in solid Al are heated at 25 kJ/g/ns over a 1 ns pulse (corresponding to 35 J/cm^2). In Fig. 2, results from a simulation (by S.F. Ng) using the 1D DISH [14] code adapted to spherical coordinates [18] are displayed. The equation of state used in the simulation is QEOS [15]. In the simulations ~ 10 Mbar pressures were obtained in the center of bubble.

Simulations in which the targets are planar with cylindrical holes parallel to the beam direction have also been carried out (by E. Henestroza) using HYDRA. The ion beam heats the walls of the cylinder, compressing the heated metal along the axis of the hole. For energy deposition of 10 J/cm^2 (a conservative estimate of NDCX-II capabilities) onto 4- μ -thick Sn foil, with a 6- μ -diameter cylindrical hole, central temperatures of 2.6 eV and maximum pressures of 1.3 Mbar were achieved.

Another class of targets that is being considered for study on NDCX-II is metallic foams. To understand the simple scaling of expansion rate, pressure and temperature evolution, and homogenization rate with foam parameters, a model consisting of solid slabs and voids has been simulated. Fig. 3 illustrates a typical simulation result (by A. Zylstra) from the DISH [14] code of a planar 30% Al foam consisting of 15 layers. The slabs were heated in 0.5 ns pulse, with a total energy deposition of 30 kJ/gm. The figure shows the initial evaporation of the slabs, followed by partial homogenization, and a macroscopic rarefaction wave propagating to the center of the slab. Foams are of interest because of their use in ICF targets as radiation converters and structural material, as well as the intrinsic physics.

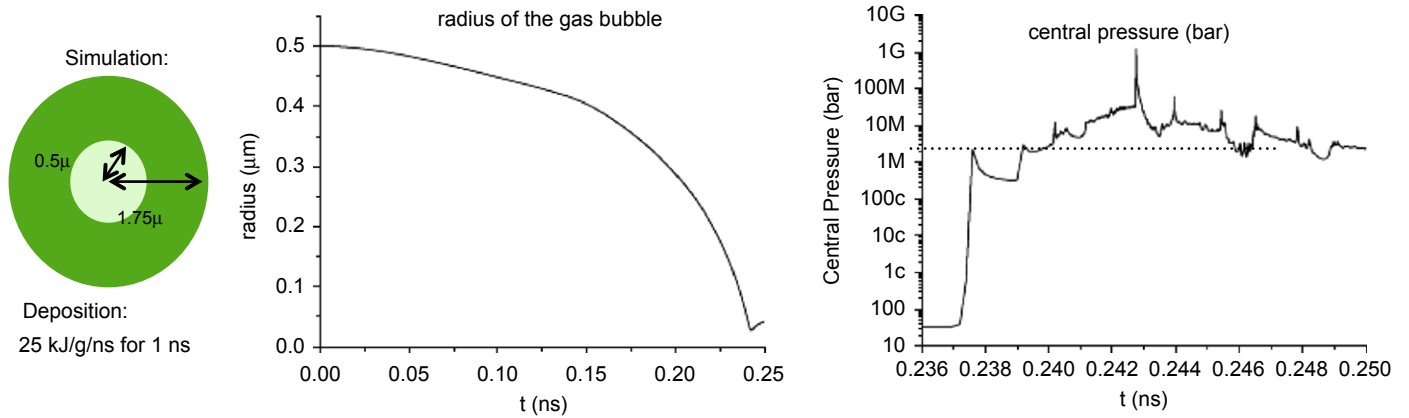


Fig. 2. Simulation (by S.F. Ng) of a spherically imploding bubble in Al for NDCX-II parameters.

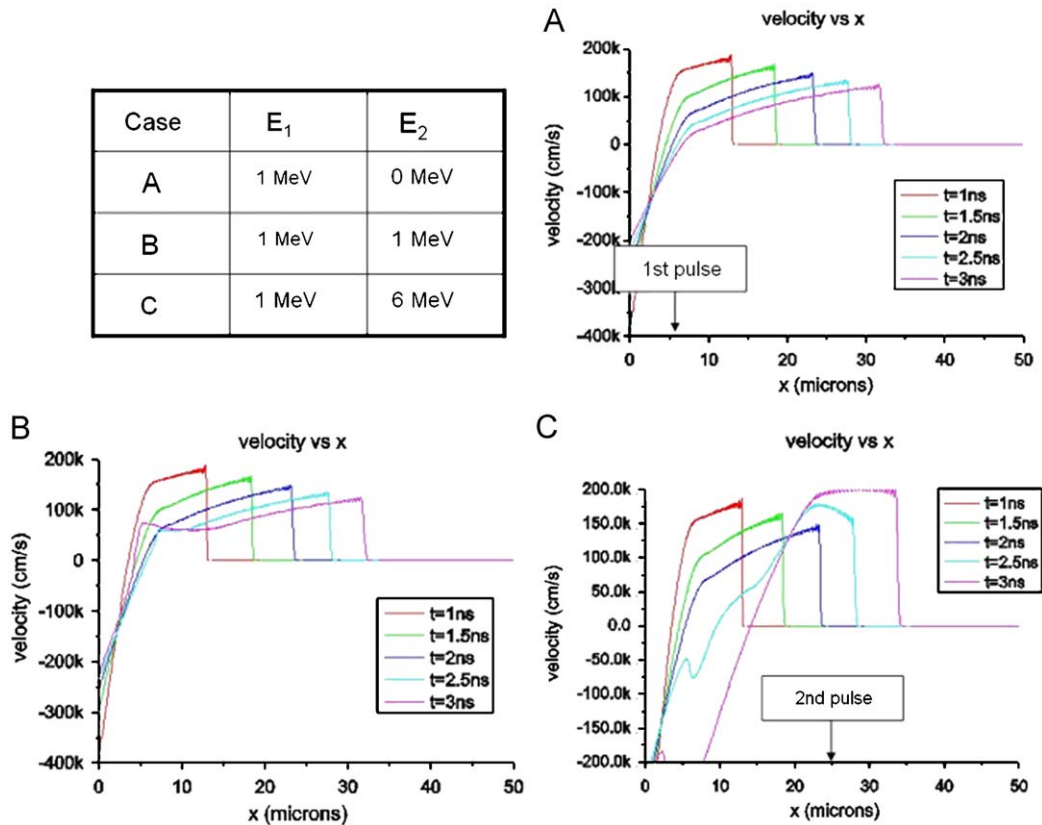


Fig. 3. Evolution of the density (ρ) of a 1D metallic foam, consisting of 15 solid layers interspersed with voids using the DISH code. (see Section 3 for simulation parameters).

4. Direct drive targets for IFE

As discussed in the introduction, direct drive targets are attractive because the energy in the driver beam is directly deposited into the ablator, minimizing the total required energy in the beam pulse. (In indirect drive, some of the energy is used to heat up and ionize the hohlraum, reducing the beam-to-capsule coupling efficiency; but the approach benefits from more uniform illumination of the capsule). With laser direct drive, the laser energy is deposited in a zone near the critical density, which, over the course of the laser pulse, increases its distance from the inwardly propagating fuel shell, so that by the end of the pulse, the laser-to-capsule coupling efficiency is small. For the case of

ion beams, the ion energy is deposited volumetrically so the ion energy can be deposited (at least initially) close to the edge of the fuel shell. If the ion energy and range were held constant, as the ablation material blows off of the capsule, the ion beam would be stopped in the blowoff material, at an increasing distance from the ablation surface, limiting its ability to accelerate the fuel shell. However by increasing the ion energy, and hence the ion range, the energy transfer can be kept high. Earlier work (see e.g. [19–21]) have taken advantage of the increasing ion energy to compensate for range shortening. Recent simulations [1] have demonstrated the effect of increasing ion range over the course of the pulse, leading to coupling efficiencies of 15%. In those simulations, the range increase came from the increasing target electron temperature. Analytical calculations [16] show that by increasing the ion energy by a larger factor than previous work (and reducing the spot size) over the course of the pulse, the coupling can increase to $\sim 25\%$. This is nearly four times the coupling efficiency of lasers, attributable to the volumetric energy deposition of ion beams, and the effect of keeping the deposition point close to the ablation front.

5. NDCX-II Targets for IFE

In addition to WDM studies described in Section 3, NDCX-II will test the efficacy of energy ramping to increase coupling efficiency that is crucial for the direct drive target concepts discussed in Section 4 above. The concept for the experiment is to compare the target performance after two ion pulses heat a planar slab of material creating a shock wave, for which the velocity can be measured at the downstream face of the slab. By comparing the results when the second pulse has the same energy as the first, to those for the case when the second pulse has a higher energy than the first, the effect of energy ramping can be demonstrated. For either case, the first pulse of the ion beam deposits energy in one ion range R (where the target is envisioned to be have a thickness that is about three times the ion range). After one hydrodynamic time (R/c_s , where c_s is the sound speed) the ablation pressure wave has propagated a distance $\sim R/c_s$, and has raised the temperature from an initial temperature T_0 to a higher temperature T_1 . Meanwhile if the second pulse is at the same ion energy, it is stopped in the outflowing plasma and does not add any energy to the ablation pressure. However, if the second pulse has a sufficiently higher ion energy and hence larger range, the second pulse energy deposition can be right behind the ablation wave, adding to the pressure and temperature T_2 of the wave, where $T_2 > T_1$. In an ion direct drive target, a temporally ramping ion energy will lead to efficient coupling of the ion beam energy into ablation pressure, which ultimately leads to an efficient acceleration of the fuel layer in the target, and thus efficient coupling of ion energy into fuel kinetic energy. In a planar experiment on NDCX-II, the coupling efficiency can be calculated by measuring the velocity of the material at the face of the target where the beam exits the slab, after the pressure wave has reached it. We have carried out simulations of these types of experiments. Energies of up to 6 MeV are assumed, achieved either by increasing the number of induction cells in the accelerator or by doubly ionizing the Li beam.

In Fig. 4, an ion pulse of length one ns and energy of 1 MeV impinges upon a 50-micron-thick slab of solid Ar at $x = 0$, creating a weak shock wave that propagates to the right. A second pulse also of duration 1 ns impinges upon the slab at time $t = 2$ ns. Snapshots of the velocity profile within the slab are shown for three different cases A, B, and C, having second pulse ion energies of 0, 1, and 6 MeV, respectively, at five different times. As can be seen from the figure, the velocity of the shock wave is not changed if the second pulse has an ion energy of 1 MeV or is not there at all

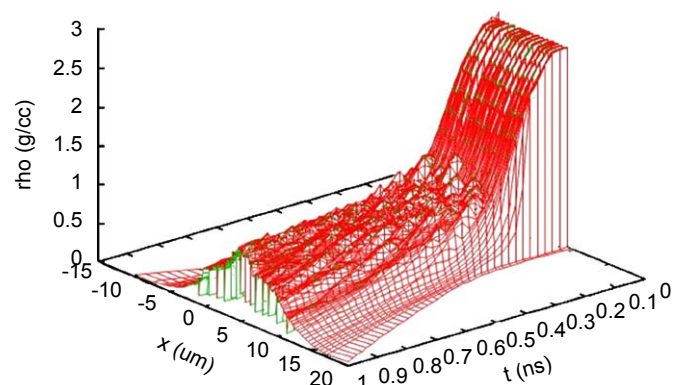


Fig. 4. Simulations (by S.F. Ng) using the DISH code of the double-pulse experiment (see Section 5 for explanation).

(0 MeV), (indicating weak coupling of the second pulse) but is greatly enhanced if the ion energy increases to 6 MeV energy, so that its increased range can keep pace with the shock front. Other simulations (not shown) indicate that a single 6 MeV pulse would produce material velocities much less than the combination of a 1 MeV and a 6 MeV pulse. Other experimental concepts including the use of a ramped pulse instead of two separate pulses, and double pulses in metallic foams have been investigated [17] and are reported elsewhere.

6. Conclusion

We have simulated a number of novel target concepts for the current NDCX-I experiment at Lawrence Berkeley National Laboratory and the planned upgrade to it, NDCX-II. Simulations suggest the metallic two-phase regime in NDCX-I can be explored. In NDCX-II, planar targets at temperature of ~ 1 eV and pressure of ~ 0.5 Mbar are predicted; cylindrical imploding bubbles will reach a few eV, and pressures greater than 1 Mbar, and spherical imploding bubbles could reach ~ 10 eV, 10 Mbar pressure. Foam homogenization, expansion and peak temperature are being modeled using “planar” foams. Droplet formation is being studied using a model that follows the evolution of a single droplet in an expanding gas.

For HIF, direct drive concepts have been proposed that have high coupling efficiency, by utilizing a ramped ion energy. NDCX-II will be able to test this key aspect of this direct drive target concept, changing ion energy to keep the ion deposition point close to ablation front. Simulations give evidence that the downstream slab velocity will give significant differences between double pulse experiments in which the energy is ramped versus the unramped case.

References

- [1] B.G. Logan, L.J. Perkins, J.J. Barnard, Phys. Plasmas 15 (2008) 072701.
- [2] Frontiers in High Energy Density Physics—The X-Games of Contemporary Science, National Academies Press, 2003.
- [3] P.A. Seidl, et al., Nucl. Instr. and Meth. A (2009), in press, doi:10.1016/j.nima.2009.03.254.
- [4] N.A. Tahir, et al., PRL 95 (2005) 035001.
- [5] N.A. Tahir, et al., Nucl. Instr. and Meth. A 577 (2007) 238.
- [6] P.K. Roy, et al., Nucl. Instr. and Meth. A (2009), in press, doi:10.1016/j.nima.2009.03.228.
- [7] P.C. Efthimion, et al., Nucl. Instr. and Meth. A (2009), in press, doi:10.1016/j.nima.2009.03.096.
- [8] F.M. Bieniossek, et al., Nucl. Instr. and Meth. A (2009), in press, doi:10.1016/j.nima.2009.03.123.

- [9] A. Friedman, et al., Nucl. Instr. and Meth. A (2009), in press, doi:10.1016/j.nima.2009.03.189.
- [10] M.M. Marinak, G.D. Kerbel, N.A. Gentile, O. Jones, D. Munro, S. Pollaine, T.R. Dittrich, S.W. Haan, Phys. Plasmas 8 (2001) 2275.
- [11] E. Lescoute, L. Hallo, B. Chimier, V.T. Tikhonchuk, D. H'ebert, J.-M. Chevalier, B. Etchessahar, P. Combis, Phys. Plasmas 15 (2008) 063507.
- [12] J. Armijo, J. Barnard, R. More, Bull. Am. Phys. Soc. 51 (2006); J. Armijo, J. Barnard, in preparation (2009).
- [13] J.J. Barnard, J. Armijo, R.M. More, A. Friedman, I. Kaganovich, B.G. Logan, M.M. Marinak, G.E. Penn, A.B. Sefkow, P. Santhanam, P. Stoltz, S. Veitzer, J.S. Wurtele, Nucl. Instr. and Meth. A 577 (2007) 275.
- [14] R.M. More, DISH User Manual, 2008, LBNL Report.
- [15] R.M. More, K.H. Warren, D.A. Young, G.B. Zimmerman, Phys. Fluids 31 (1988) 3059.
- [16] B.G. Logan, Exploring a Unique Vision for HIF, preprint, January 2008.
- [17] S.F. Ng, S. Veitzer, J.J. Barnard, P.T. Leung, S.S. Yu, in preparation (2009).
- [18] S.F. Ng, et al., Nucl. Instr. and Meth. A (2009), doi:10.1016/j.nima.2009.03.088.
- [19] K.A. Long, N.A. Tahir, Phys. Rev. A 35 (1987) 2631.
- [20] G.O. Allshouse, R.E. Olson, D.A. Callahan-Miller, M. Tabak, Nucl. Fusion 39 (1999).
- [21] M. Tabak, D. Callahan-Miller, Phys. Plasmas 5 (1998) 1895.